

#### **MALAYSIAN JOURNAL OF ANALYTICAL SCIENCES**



Journal homepage: https://mjas.analis.com.my/

## **Research Article**

Density functional theory (DFT) study of reduced graphene oxide magnetite nanoparticles (rGO-MNP) as a potential electrocatalyst for oxygen-reduction reaction

Ainul Mardhiah Mansor<sup>1</sup>, Farhanini Yusoff<sup>1\*</sup>, Suhaila Sapari<sup>2</sup>, and Fazira Ilyana Abdul Razak<sup>3</sup>

Received: 13 August 2024; Revised: 17 November 2024; Accepted: 18 November 2024; Published: 10 February 2025

#### Abstract

In the relentless pursuit of ground-breaking advancements in clean energy, this study unveils a an electrocatalyst—reduced graphene oxide integrated with magnetite nanoparticles (rGO-MNP)—designed to revolutionize the oxygen reduction reaction (ORR). Through sophisticated density functional theory (DFT) simulations, we demonstrate how the hybridization of MNP with rGO leads to profound modifications in electronic properties, unlocking unprecedented enhancements in catalytic activity and electron transport. The composite exhibits extraordinary stability, as evidenced by a binding energy of -1036.96 kJ/mol, while its interaction energy of -389.29 kJ/mol signals a thermodynamically advantageous structure. Molecular electrostatic potential (MEP) mapping reveals a rich interplay of electron-dense and deficient regions, crucial for optimizing ORR mechanisms. Additionally, the narrow HOMO-LUMO gap of 0.173 eV underscores the material's high reactivity and optimal charge transfer dynamics. These computational insights affirm rGO-MNP as a next-generation electrocatalyst, offering not only exceptional stability and efficiency but also the potential to drive transformative improvements in sustainable energy technologies. This work establishes a robust foundation for the development of efficient, durable, and scalable ORR catalysts, opening avenues for impactful applications in fuel cells and clean energy systems.

**Keywords:** oxygen reduction reaction, reduced graphene oxide, magnetite nanoparticles, density functional theory, electrocatalyst

#### Introduction

The current electricity generation system faces significant challenges in meeting the growing demand for clean and reliable power [1, 2]. Fossil fuels are a consistent source of electricity but are costly. However, the current problem is not necessarily a lack of fossil fuels, but the environmental and economic burdens associated with their continued use to generate electricity [3, 4, 5]. Fuel cells are a sustainable and cost-competitive alternative that can meet our growing energy demand [1, 2, 4, 6, 7]. Oxygen reduction reactions (ORR) are the cornerstone of electrochemical energy conversion in devices like fuel cells [1, 7, 8]. They represent the heart of the process where chemical energy stored in fuels is transformed into usable electrical energy. An ORR involves two simultaneous processes: oxidation and reduction. During ORR, the electron donor loses electrons, increasing its oxidation state. Conversely, the electron acceptor gains electrons, decreasing its oxidation state. This transfer of electrons releases energy, which manifests as electricity in the fuel cells. Fuel cell functions on the coupled principles of oxidation and reduction at anode and cathode electrodes. At the anode, the fuel undergoes oxidation, releasing electrons and protons (often in the form of hydrogen ions) into the electrolyte. These released electrons travel through an external circuit, generating an electric current. When electrons reach the cathode, they participate in the ORR [6, 9]. Here, oxygen gas from the air is the electron acceptor, gaining electrons and protons from the electrolyte to form water as the product. The efficiency of the ORR at the cathode significantly impacts the overall performance of the

<sup>&</sup>lt;sup>1</sup>Faculty of Marine Science and Environment, Universiti Malaysia Terengganu, 21030 Kuala Nerus, Terengganu, Malaysia <sup>2</sup>Department of Chemical Sciences, Faculty Science and Technology, Universiti Kebangsaan Malaysia, 43600 UKM Bangi, Selangor, Malaysia

<sup>&</sup>lt;sup>3</sup>Chemistry Department, Faculty of Science, Universiti Teknologi Malaysia, 81310 Skudai, Johor, Malaysia

<sup>\*</sup>Corresponding author: farhanini@umt.edu.my

fuel cell [2, 4, 6, 10].

Electrocatalysts play a crucial role in driving the ORR. However, several limitations hinder the widespread application of ORRs. One major challenge is cost [1], [4]. Many high-performance electrocatalysts rely on precious metals like platinum (Pt), which are expensive and scarce, making them a barrier to large-scale adoption and widespread use of ORR technologies [7, 10]. Researchers strive to develop electrocatalysts with even higher ORR activity, which translates to better efficiency in converting oxygen to usable energy [9].

Two promising materials have emerged in the quest for better ORR electrocatalysts: reduced graphene oxide (rGO) and magnetite nanoparticles (MNP) [2]. The rGO boasts exceptional properties for ORR electrocatalysis, i.e., high electrical conductivity due to its planar and honeycomb lattice structure, which facilitates efficient electron transfer during ORR, maximizing reaction rates and performance [2, 7], [10, 11]. Additionally, its large surface area, stemming from its single atomic layer thickness, provides a vast expanse for oxygen molecules to interact with, maximizing the number of active sites and promoting efficient ORR activity [11, 12]. Yusoff et al. reported that the interaction between iron oxide (Fe<sub>3</sub>O<sub>4</sub>) and carbon-based materials significantly enhances the properties of the resulting composite. This interaction leads to notable improvements in magnetic and catalytic activities, making the composite more effective for various applications, including catalysis. Their findings demonstrated that the chemical functionalisation and decorating of carbon nanotubes with Fe<sub>3</sub>O<sub>4</sub> nanoparticles at varying voltages reduced their electrical resistance from 3923 to 1266  $\Omega$ m. This outcome suggested that combining these two nanoparticles facilitates research on the conductive characteristics of carbon [2]. Finally, the presence of various oxygen-containing functional groups (e.g., hydroxyl, carboxyl) on rGO's surface allows for tailored surface chemistry, enabling researchers to fine-tune its interaction with oxygen molecules and further enhance ORR performance [1, 2, 12, 13].

MNP offers a compelling alternative to traditional precious metal catalysts for ORR applications. Its abundance and low cost make it readily available and economically attractive for large-scale implementation [1, 14]. MNPs have garnered significant attention due to their superparamagnetic properties, high coercivity, and low Curie temperature [11]. Furthermore, MNP exhibits inherent catalytic ORR activity, providing a solid foundation for further enhancement. This intrinsic activity and the potential for synergistic effects when combined with materials like rGO opens exciting avenues for material design

and engineering. rGO's high electrical conductivity significantly improves electron transfer during ORR, while MNP provides the essential active sites for the reaction [2, 14]. This interplay between the two materials has the potential to unlock significantly improved ORR performance.

Researchers are enthralled by the potential of combining rGO and MNP to create composite ORR electrocatalysts. These composites can leverage the strengths of both materials, offering enhanced activity due to the synergistic effect of rGO's conductivity and MNP's intrinsic activity, potentially leading to superior ORR performance compared to individual materials [2, 14].

Additionally, the rGO support structure can improve the catalyst durability by protecting the MNP from degradation, extending the device's lifespan. Their applications extend beyond opening doors for advancements in batteries, electrolysis, and other sustainable energy solutions [2, 12, 14]. While both rGO and MNP hold promise for ORR electrocatalysis, further research is ongoing to optimize their performance and address any limitations. However, their unique properties and potential for synergistic effects in composites make them promising candidates for the future of clean energy technologies [3]. Building upon the potential of rGO and MNP as individual ORR electrocatalysts, this research delves into their synergistic potential by investigating rGO-MNP composite materials using DFT calculations.

This research used DFT calculations to find the optimal arrangement for MNP on a specific rGO model. Studying DFT involves the visualization of electronic properties using tools like Molecular Electrostatic Potential (MESP) maps or HOMO-LUMO gap analysis to obtain clear images of electron density distribution, allowing researchers to identify areas on the catalyst likely to enhance ORR activity, as demonstrated by Al-Bagawi et al. [11]. Experimentally, measuring these properties requires extensive spectroscopic analysis, which may not always capture the dynamic behaviour of electrons in real-time or at the atomic level [2].

We acknowledge that other rGO models exist, but focusing on this allows us to concentrate on how oxygen molecules interact with the supported metal particles and how this interaction changes depending on the electrical potential (electrode potential) applied. It is important to note that using clusters of atoms, both isolated and supported, is a common approach to studying reaction mechanisms in catalysts, and the complexity of these clusters could vary from just one atom to several [9]. DFT calculations have become essential in unlocking the

full potential of rGO-MNP composites for ORR catalysis. By offering a microscopic perspective and guiding material design strategies, DFT calculations pave the way for developing next-generation catalysts that can revolutionize clean energy applications such as fuel cells.

## Materials and Methods DFT studies using Gaussian 09 Software

The desktop operates on a 64-bit operating system with an x64-based processor, 4 GB of installed memory, and 3.87 GB of RAM. Molecular optimization was conducted using DFT with the B3LYP method and the Gaussian 09 program package software. All calculations were performed in a vacuum, employing the 6-31G (d,p) basis set for carbon, hydrogen, and oxygen atoms. The GEN keyword with the LANL2DZ basis set was used for metal atoms, such as iron (Fe). Additionally, BSSE correction was applied using the counterpoise keyword to accurately determine the interaction energy for the rGO-MNP system. The counterpoise correction was applied with counterpoise=2 to account for the interaction between rGO and MNP fragments. The geometry optimization of the molecule was carried out without imposing any symmetry constraints [1, 11, 15]. The resulting data was processed and visualized for further analysis using the GaussView 6 software, allowing a deeper understanding of the system's behaviour. In addition to the simulations, researchers also generated maps depicting the distribution of electrical charges around the molecules (called MESP maps) [11, 16]. Various physical properties were extracted from the calculations, including the total energy of the molecule, its overall propensity to lean positive or negative in an electric field (total dipole moment), and the energy gap between its most reactive electron donor orbital (HOMO) and acceptor orbital (LUMO). These additional details provide valuable insights into the molecule's behaviour [11, 16].

# Results and Discussion Geometry optimization

A detailed description of how the model molecules were put together is essential to ensure transparency and reproducibility of the research. The model was built using GaussView 6 software. **Figure 1** demonstrates the optimized constructed model molecules of GO, rGO, and MNP. The structure of GO and rGO shows a hexagonal lattice typical of graphene, composed of carbon atoms (grey spheres) bonded in a honeycomb pattern [1, 11]. Several

oxygen atoms (red spheres) are attached to the graphene lattice. These are part of various oxygencontaining functional groups such as hydroxyl (-OH), carbonyl (C=O), and epoxy (-O-) groups that are distributed across the graphene lattice, providing sites for oxygen molecule adsorption and reduction [13]. These functional groups significantly influence the electronic properties of rGO, enhancing its catalytic efficiency [2]. Hydrogen atoms (white spheres) are also present and attached to carbon atoms, completing the functional groups. The rGO typically has fewer oxygen groups than GO, which is heavily functionalized with oxygen-containing groups. The oxygen functional groups on the graphene surface can serve as active sites for interaction with other molecules or ions, potentially contributing to catalytic activity. The molecular model in Figure 1(c) represents a cluster of magnetite featuring iron (Fe) and oxygen (O) atoms. The Fe-O bond lengths of approximately 1.72 Å and Fe-O-Fe bond angles of 109° indicate the tetrahedral coordination typical of the spinel structure, which is the same as reported by Al-Bagawi et al. [11].

These structural features provide active sites for the adsorption and reduction of oxygen molecules, which is crucial for the ORR. The stable coordination environment enhances the durability and catalytic efficiency of the magnetite component in the composite catalyst with rGO. Figure 2 shows the molecular structure of rGO functionalized with an iron oxide (Fe<sub>3</sub>O<sub>4</sub>). The carbon backbone of the rGO features hydroxyl (C-O bond length: 1.42 Å), carbonyl (C=O bond length: 1.37 Å), and epoxy groups (C-C bond length: 1.43 Å), with typical bond angles around 120°. The iron oxide cluster is bonded to the rGO, with a Fe-O bond length of approximately 1.72 Å, shorter than 2.00 Å reported by Jiang et al. [17], indicating stronger bonding interactions that may enhance stability. Tetrahedral magnetite was detected attached to the planar rGO on C20 and C18, which is a middle-like position of the model composite, in compliance with Al-Bagawi et al. and Vinogradov et al. [1, 11]. These structural features provide multiple active sites for the adsorption and reduction of oxygen molecules during the ORR. The synergistic effect of combining a conductive carbon-based material with a catalytic metal oxide enhances electron transfer processes, contributing to improved ORR performance.

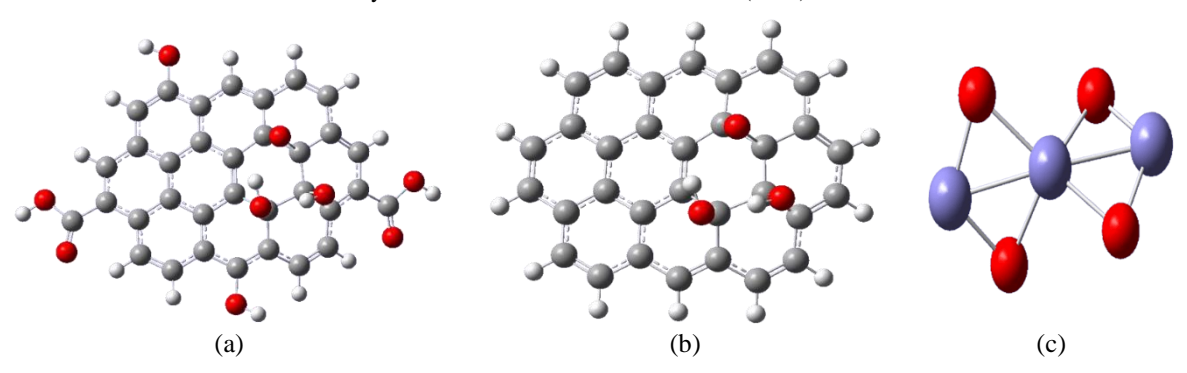


**Figure 1.** Structure of the optimized model catalysts: (a) GO, (b) rGO at the level of B3LYP/6-31G (d.p), and (c) MNP. Gray spheres- carbon, red spheres- oxygen, white spheres- hydrogen, blue spheres-the studied metal (Fe) at the level of B3LYP/GEN (LANL2DZ)

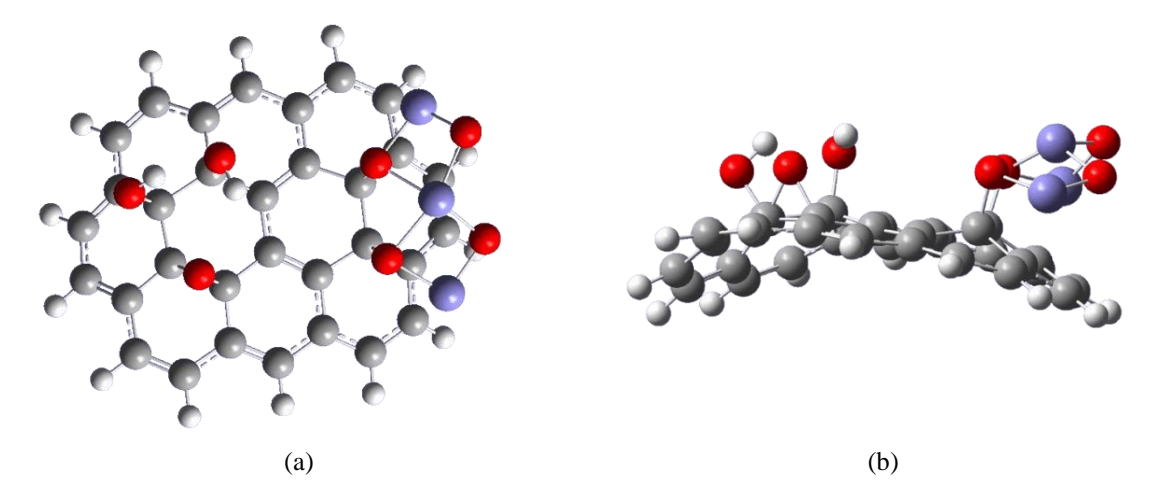


**Figure 2.** Structure of the optimized model catalysts: (a) Top and (b) side-view of optimized structures of rGO-MNP catalyst, at the level of B3LYP/GEN (LANL2DZ)

### **Binding energy**

Calculations were performed to determine the impact of functionalizing reduced graphene oxide with a ferromagnetic material on its electronic and physical properties using DFT at the B3LYP/GEN (LANL2DZ) [15]. Binding energy calculation is a crucial aspect of DFT studies and provides valuable insights into the stability and interaction strength between molecules or between a molecule and a surface. The binding energy (E<sub>binding</sub>) is the energy required to disassemble a compound into its components. For a system consisting of an adsorbate, magnetite nanoparticle, and a substrate, the reduced graphene oxide is given by Equation (1):

$$E_{binding} = E_{total} - (E_{adsorbate} + E_{substrate})$$
 (Eq. 1)

where  $E_{total}$  is the total energy of the system with the magnetite nanoparticle bound to the reduced graphene oxide,  $E_{adsorbate}$  is the energy of the isolated magnetite nanoparticle, and  $E_{substrate}$  is the energy of the isolated reduced graphene oxide [4, 6, 18].

The calculation process involves several steps. First, the geometries of reduced graphene oxide and magnetite nanoparticles are optimized separately to find their most stable configurations, minimizing energy for atomic positions. Next, the total energies of these optimized structures are calculated. The magnetite nanoparticles are then placed on the substrate surface, and the geometry of the combined system is optimized to find its total energy [4, 18]. The resulting binding energy of -1,036.96 kJ/mol indicates a highly exothermic and stable interaction, suggesting that the adsorbed species are strongly bound to the reduced graphene oxide magnetite surface. This binding energy is significantly lower than values reported by Al-Bagawi et al., where binding energies around -14,000 kJ/mol indicated weaker adsorption on similar graphene-iron oxide composites [11]. The lower binding energy highlights enhanced interaction strength and stability, making this composite more promising than previously studied materials for ORR applications [19].

This binding energy directly measures the strength of the interaction between the rGO and the MNP involved in the ORR process. The pronounced negative binding energy observed in the ORR study of rGO-MNP signifies a few pivotal aspects. Primarily, it indicates robust adsorption, ensuring effective anchoring of oxygen molecules or intermediates on the catalyst surface. This high binding energy denotes the formation of a highly stable complex, which is advantageous for catalytic processes as it facilitates efficient interaction between active sites and reactants, potentially lowering activation energy and enhancing reaction kinetics [6].

Furthermore, the stability afforded by such strong binding interactions suggests a reduction in catalyst degradation over time, which is critical for the practical application of catalysts in fuel cells and other electrochemical devices [11]. Additionally, this robust interaction promotes efficient electron transfer to the adsorbed oxygen species, a crucial step in the ORR mechanism that contributes to enhanced catalytic performance and overall efficiency [20, 21].

In summary, the binding energy of -1,036.96 kJ/mol highlights the excellent potential of reduced graphene oxide magnetite as an electrocatalyst for ORR, emphasizing its strong adsorption capacity, stability, and enhanced catalytic performance, making it a promising material for use in high-performance, durable, and cost-effective electrochemical devices.

### **Interaction energy**

We employed a rigorous computational setup to ensure the accuracy of the interaction energy calculation. The B3LYP/GEN (LANL2DZ) was chosen for its reliability in modelling electronic interactions in composite materials [15]. Additionally, we applied the Basis Set Superposition Error (BSSE) correction using the counterpoise method. This correction is crucial for eliminating the artificial stabilization effects that arise when basis sets of interacting fragments overlap. By including BSSE

correction, we obtain a more accurate representation of the true interaction energy between rGO and MNP [15, 22].

Regarding binding energy calculations, the total energy differences include all interactions, such as covalent bonds, where BSSE correction is generally less critical. Consequently, the counterpoise keyword is applied only to interaction energy calculations because these are more affected by basis set overlap errors. These computational methodologies are widely accepted in the field and are essential for obtaining reliable data. **Table 1** includes the raw (uncorrected) and BSSE-corrected interaction energy values in the supplementary materials to underscore significance of BSSE correction in our results. This transparency allows readers to observe the direct impact of BSSE correction on the calculated interaction energies. The calculated interaction energy, validated by these rigorous computational approaches, provides a credible basis for discussing the stability and catalytic potential of the rGO-MNP composite.

In this study, the interaction energy of the rGO-MNP is calculated to elucidate the strength of interactions between its components. The interaction energy (E<sub>interaction</sub>) is determined using Equation (2):

$$E_{interaction} = E_{rGO-MNP} - (E_{rGO} + E_{MNP})$$
 (Eq. 2)

where  $E_{complex}$  represents the total energy of rGO-MNP,  $E_{component1}$ , and  $E_{component2}$  are the energy of the individual components, rGO and MNP [19].

**Table 1** indicates the energy for GO, rGO, MNP, and rGO-MNP systems. It presents optimized energy values for each system. BSSE correction energy is included only for interaction energy calculations, specifically in the rGO-MNP system. Binding energy values are shown without BSSE correction.

<b>Table 1.</b> Energies for	GO, rGO, MNP	and rGO-MNP
------------------------------	--------------	-------------

Samples	Optimized Energy (kJ/mol)	BSSE Correction Energy (kJ/mol)	Binding Energy (kJ/mol)	Interaction Energy (kJ/mol)
GO	-5202937.043	NA	NA	NA
rGO	-3819457.43	-3818986.74	NA	NA
MNP	-1761479.677	-1761577.06	NA	NA
rGO-MNP	-5580953.094	-5580953.09	-1,036.96	-389.29

The interaction energy of -389.29 kJ/mol for the rGO-MNP catalyst proves a significant exothermic interaction between the rGO and MNP [19]. This substantial negative interaction energy indicates that the formation of the rGO-MNP composite is thermodynamically favourable, leading to a stable and robust structure. The stability of the catalyst is crucial for its performance in catalytic applications, especially in ORR, where maintaining the structural integrity of the catalyst is essential under operational conditions. Stability in this context means that the rGO-MNP composite is less likely to undergo degradation, deformation, or phase separation during the catalytic process [11]. A stable catalyst ensures that the active sites necessary for the ORR remain intact and accessible, leading to sustained catalytic activity over time [19]. The robust interaction between rGO and MNP means that the composite can withstand the harsh conditions typically encountered during ORR, such as high temperatures, acidic or basic environments, and continuous reaction cycling. The exothermic nature of the interaction suggests that the rGO-MNP composite is held together by strong binding forces, including van der Waals interactions, electrostatic attractions, and potentially covalent bonding [23, 24]. These interactions collectively enhance the structural stability of the composite. In the context of the ORR, this stability is beneficial because it ensures that the active sites remain accessible and intact during the reaction, which is critical for sustained catalytic activity. A stable catalyst minimizes the risk of deactivation or morphological changes that could otherwise hinder the ORR process.

The strong interaction between rGO and MNP stabilizes the composite and influences its electronic properties, enhancing the catalyst's ability to facilitate the ORR [25]. The interaction energy of -389.29 kJ/mol suggests that the rGO-MNP catalyst has a well-defined electronic structure that can effectively adsorb and activate oxygen molecules, a key requirement for the ORR. The adsorption of oxygen molecules onto the catalyst surface is a crucial step in the reaction mechanism. The enhanced electronic interaction between rGO and MNP likely improves the electronic conductivity and charge transfer properties of the catalyst, boosting its catalytic efficiency, implying that the catalyst remains structurally stable and retains high catalytic activity, promoting efficient oxygen reduction.

In summary, the interaction energy of -389.29 kJ/mol for the rGO-MNP catalyst highlights a strong and stable interaction between rGO and MNP, which is critical for its performance in the ORR. This interaction only enhances the structural stability of the catalyst and optimizes its electronic properties,

facilitating efficient oxygen molecule adsorption and activation.

In conclusion, the contrasting values of binding energy and interaction energy in the rGO-MNP composite provide essential insights into its structural design and stability, both critical for its role in ORR catalysis. The highly exothermic binding energy of  $-1,036.96 \, \text{kJ/mol}$  signifies a robust attachment of MNP to the rGO surface, indicating a strong anchoring mechanism that prevents MNP detachment. This firm binding ensures that the active sites remain intact and functional during catalytic cycles, which is vital in maintaining consistent performance in ORR applications, especially under the demanding conditions of electrochemical cycling.

In contrast, the interaction energy of -389.29 kJ/mol highlights a more flexible stabilizing effect between the rGO and MNP components. Although a lower value, it reflects the van der Waals and electrostatic forces that help maintain the composite's structural cohesion without overly rigid confinement. Such a balance allows the composite to accommodate slight rearrangements, which may enhance resilience to mechanical stress during extended catalytic use. The distinction between binding and interaction energy is crucial in the composite's overall performance. The substantial binding energy anchors the catalytic sites firmly, reducing the likelihood of degradation, while the moderated interaction energy allows for adaptive flexibility, balancing stability with endurance. Together, these properties establish the rGO-MNP composite as a highly durable and effective ORR electrocatalyst, demonstrating robust attachment of active components and the adaptability needed for long-term catalytic activity. This dual stabilityadaptability profile makes the rGO-MNP composite an outstanding candidate for advanced ORR applications in energy devices where durability and performance are paramount.

### **Dipole moment analysis**

The total dipole moment (TDM) of the rGO-MNP catalyst was calculated to provide insights into its electronic properties and behaviour in the ORR. The dipole moment, indicative of the charge distribution within the composite, is critical in influencing the adsorption characteristics of oxygen molecules on the catalyst surface [11]. The analysis of the TDM for the catalysts under study—GO, rGO, MNP, and the rGO-MNP—reveals significant insights into their electronic properties and potential catalytic activity for the ORR. The TDM is as follows: GO exhibits a dipole moment of 5.2152 Debye, rGO shows a reduced dipole moment of 3.6887 Debye, MNP has a minimal dipole moment of 0.5125 Debye (slightly

higher than reported by Al-Bagawi et al. [11]), and the rGO-MNP composite has a substantial dipole moment of 8.9872 Debye (refer to **Table 2**). The rGO-MNP composite exhibits a notably high TDM, indicating strong polarization effects within the composite material. The high TDM suggests that the rGO-MNP catalyst creates an intense electric field at its surface, enhancing its ability to interact and polarize with oxygen molecules. Oxygen molecules (O<sub>2</sub>) are inherently nonpolar, but a strong electric field due to a high dipole moment can induce a polarization in these molecules, making them more reactive. This polarization helps weaken the O=O double bond in the oxygen molecule, facilitating its activation.

As a result, oxygen molecules more readily undergo the reduction process, which is essential for effective ORR. This improved interaction facilitates more effective adsorption of oxygen molecules onto the catalyst surface, which is crucial for the ORR. The enhanced polarization reduces activation energy for the reaction and ensures that more oxygen molecules are available, resulting in higher catalytic activity and efficiency. In contrast, the rGO catalyst with a TDM of 3.6887 Debye and MNP with a TDM of 0.5125 Debye show lower polarization effects than the rGO-MNP composite. The lower TDM values indicate weaker polarization and less effective interaction with oxygen molecules [9]. Although rGO provides a reasonable dipole moment that can contribute to ORR, MNP shows minimal polarization with its low TDM. The individual catalytic performance of these materials is not as enhanced as the rGO-MNP composite.

The high TDM of the rGO-MNP composite suggests that the synergistic effect of combining rGO with MNP significantly boosts the polarization effects compared to either material alone. The improved polarization enhances the active sites for oxygen reduction, making the rGO-MNP composite a more effective catalyst for ORR. The results from the TDM analysis highlight the potential of the rGO-MNP composite to provide superior catalytic performance, driven by its strong polarization capabilities. In conclusion, the high TDM observed in the rGO-MNP composite underscores its enhanced capability for ORR compared to rGO and MNP individually. This enhanced dipole moment contributes to better oxygen molecule interaction, lower activation energy, and improved catalytic efficiency, making the rGO-MNP composite a promising candidate for applications requiring effective oxygen reduction.

#### Frontier molecular orbital (FMO)

A smaller HOMO-LUMO gap indicates higher reactivity, which is advantageous for catalytic processes [18]. This study analyses the HOMO-

LUMO gaps of GO, rGO, MNP, and the rGO-MNP composite to evaluate their potential as ORR catalysts. **Table 2** shows the resulting energy of the HOMO-LUMO gap.

Figure 3 depicts the HOMO (top image) and LUMO (bottom image) distributions of GO, rGO, MNP, and rGO-MNP, along with their respective energy gaps. The HOMO-LUMO gap for GO is 1.380 eV. The HOMO electron density is primarily localized around the oxygen-containing functional groups, indicating regions of high electron availability essential for donating electrons during catalytic reactions. The LUMO electron density is more delocalized across the graphene sheet, especially around the edges and defect sites, suggesting potential sites for electron acceptance. This moderate HOMO-LUMO gap suggests that GO has decent reactivity but might not be the most efficient catalyst for ORR. The localized electron density around oxygen groups facilitates interactions with oxygen molecules, enhancing the ORR process. The HOMO-LUMO gap for rGO is slightly higher at 1.738 eV. The HOMO electron density is more spread out than GO, indicating increased conductivity and better electron mobility. The LUMO remains localized around residual oxygen functionalities, which could act as active sites for electron acceptance during ORR. Despite the larger gap implying lower reactivity, the increased conductivity of rGO aids in efficient electron transfer, which could enhance ORR performance. MNP exhibits a much smaller HOMO-LUMO gap of 0.226 eV, indicating high reactivity. The HOMO electron density is concentrated around the iron atoms, suggesting potential for effective electron donation. The LUMO also has electron density focused around the iron atoms, facilitating electron transfer processes. This small gap makes MNP highly effective for ORR, with active sites crucial for reducing oxygen molecules, enhancing ORR efficiency.

The rGO-MNP composite exhibits a remarkably small HOMO-LUMO gap of 0.17276 eV, the smallest among the materials studied, indicating high reactivity crucial for catalytic processes like ORR. The distribution of HOMO electron density across both rGO and MNP components suggests a synergistic interaction that enhances the overall electronic properties of the composite. The synergistic effect arises from the combination of rGO's excellent electrical conductivity and MNP's catalytic activity. This combination leads to a highly reactive material and is efficient in facilitating electron transfer, a critical aspect of the ORR process. The delocalization of LUMO electron density across the composite material further facilitates efficient electron transfer. Efficient electron transfer is vital in ORR, where the transfer of electrons to oxygen molecules is a key step.

**Table 2.** Calculated physical parameters of TDM as Debye and band gap energy as eV for GO, rGO, MNP and rGO-MNP using B3LYP/6-31G(d,p) and GEN (LANL2DZ)

Structure	TDM (Debye)	Energy gap (eV)
GO	5.2152	1.380
rGO	3.6887	1.738
MNP	0.5125	0.226
rGO-MNP	8.9872	0.173

The rGO-MNP composite's ability to facilitate this process effectively reduces oxygen molecules, enhancing the overall catalytic performance.

The high conductivity of rGO provides a pathway for rapid electron movement, while the catalytic sites on MNP are strategically positioned to interact with the oxygen molecules, improving ORR kinetics. Compared to its individual components, the rGO-MNP composite outperforms rGO and MNP alone. While rGO offers excellent conductivity, its larger HOMO-LUMO gap (1.738 eV) limits its reactivity. On the other hand, MNPs have high reactivity (0.226 eV HOMO-LUMO gap) but suffer from potential agglomeration and lower conductivity. The composite overcomes these limitations by combining the strengths of both materials, resulting in a highly reactive, stable, and efficient catalyst that transfers electrons.

In summary, the rGO-MNP composite is an advantageous catalyst for ORR due to its synergistic interaction, efficient electron transfer, and abundant active sites. These properties collectively enhance the catalytic performance, making the composite a superior choice for ORR applications compared to its components. Combining rGO's conductivity and MNP's catalytic activity ensures a highly reactive and durable catalyst, improving efficiency and longevity in practical ORR applications, making the rGO-MNP composite an excellent candidate for advanced fuel cell technologies and other ORR-based systems.

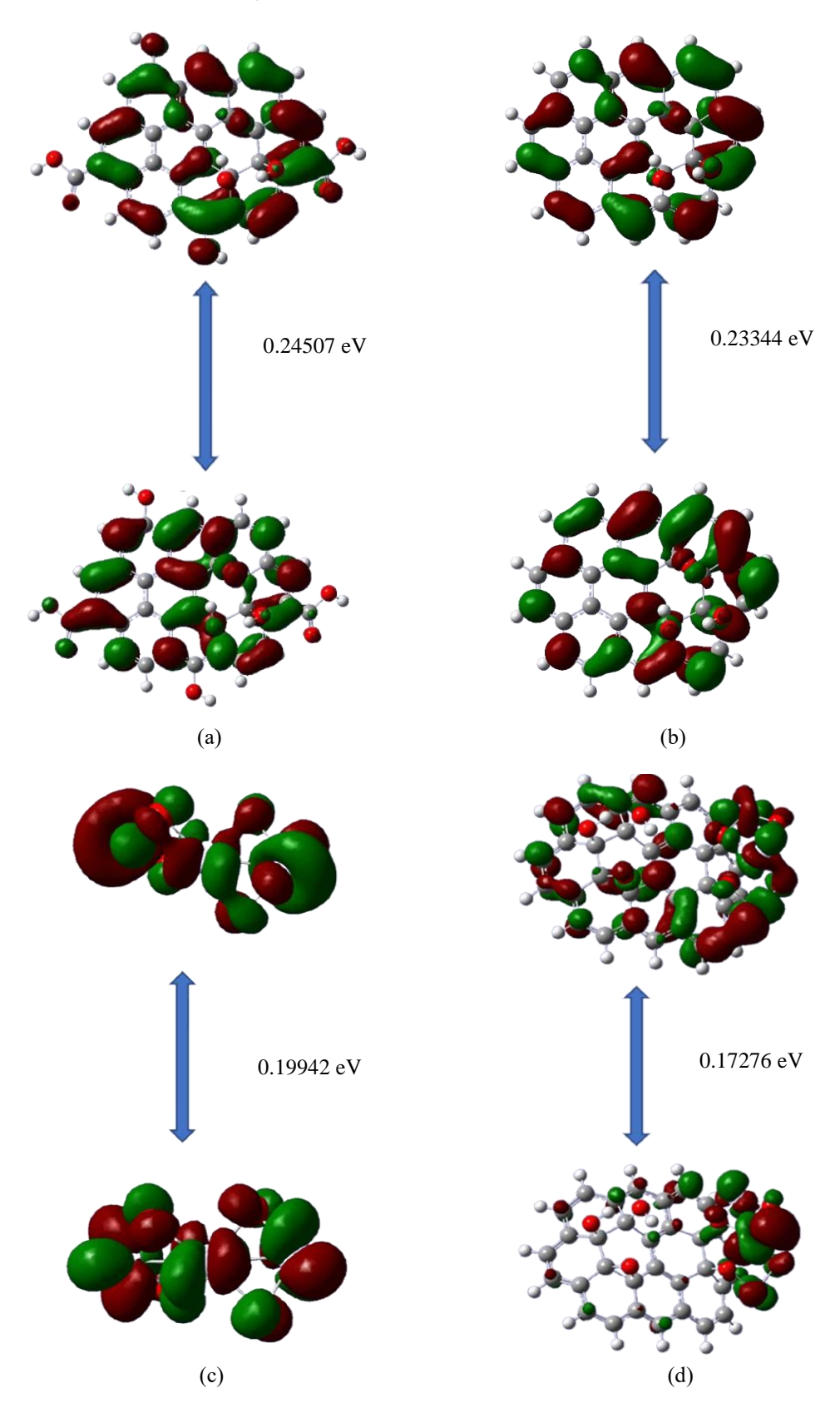
### Molecular electrostatic potential (MEP) maps

MEP is a three-dimensional function that represents the electrostatic potential energy experienced by a test charge (usually a proton) due to the electrons and nuclei of a molecule. It provides insights into the charge distribution within the molecule. MEP is often visualized using color-coded maps on the molecular surface. Regions with negative potential (typically red) indicate electron-rich areas, and the regions with positive potential (typically blue) indicate electron-deficient areas, showing areas where the electron density is lower. The yellow and green areas represent regions of intermediate electrostatic potential, lying between the extremes of positive (blue) and negative (red) potential. These regions indicate a balanced

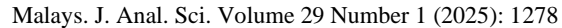
distribution of electron density. Yellow and green regions (intermediate potential) often correspond to areas where the carbon atoms are part of the aromatic graphene backbone but not directly bonded to oxygencontaining functional groups. These areas might be less reactive compared to the strongly polarized regions but still play a role in the overall interaction with adsorbates during catalytic processes [11, 16, 26, 27]. The MEP maps in Figure 4 provide valuable insights into the electronic distribution and potential reactive sites of the catalysts: GO, rGO, MNP, and the rGO-MNP composite. These maps, calculated using DFT with the B3LYP/6-31G(d,p) and GEN (LANL2DZ) basis set for metal atoms, highlight regions of positive and negative electrostatic potential, which correlate with nucleophilic and electrophilic sites, respectively.

The DFT-calculated MEP maps for GO, rGO, MNP, and rGO-MNP reveal significant insights into their electrostatic properties. In Figure 4(a), the MEP map for GO displays regions of both positive and negative potential, with negative potential (red areas) primarily localized around oxygen-containing functional groups like epoxy and hydroxyl groups, indicating electronrich sites that can potentially act as adsorption sites for oxygen molecules during the ORR. The positive potential regions are typically found around carbon atoms not bonded to oxygen-containing functional groups. These electron-deficient sites are crucial for interacting with negatively charged species or nucleophiles.

In contrast, as shown in Figure 4(b), the MEP map of rGO shows red, blue, yellow, and green regions, but with less pronounced negative potential regions (red) due to the reduction process that removes some oxygen functional groups. The blue regions (positive potential) are more prominent in rGO than GO, indicating an increase in electron-deficient sites. The MNP map in Figure 4(c) reveals distinct positive and negative potential regions, with positive potential (blue areas) associated with Fe atoms, indicating electron-deficient sites. The negative potential regions associated with O atoms indicate electron-rich sites. The yellow and green regions are less prominent, indicating a more polarized distribution of electrostatic potential in MNP. This polarization is



**Figure 3.** DFT calculated HOMO (top image) and LUMO (bottom image) of (a) GO, (b) rGO, (c) MNP, (d) rGO-MNP alongside their respective energy gaps



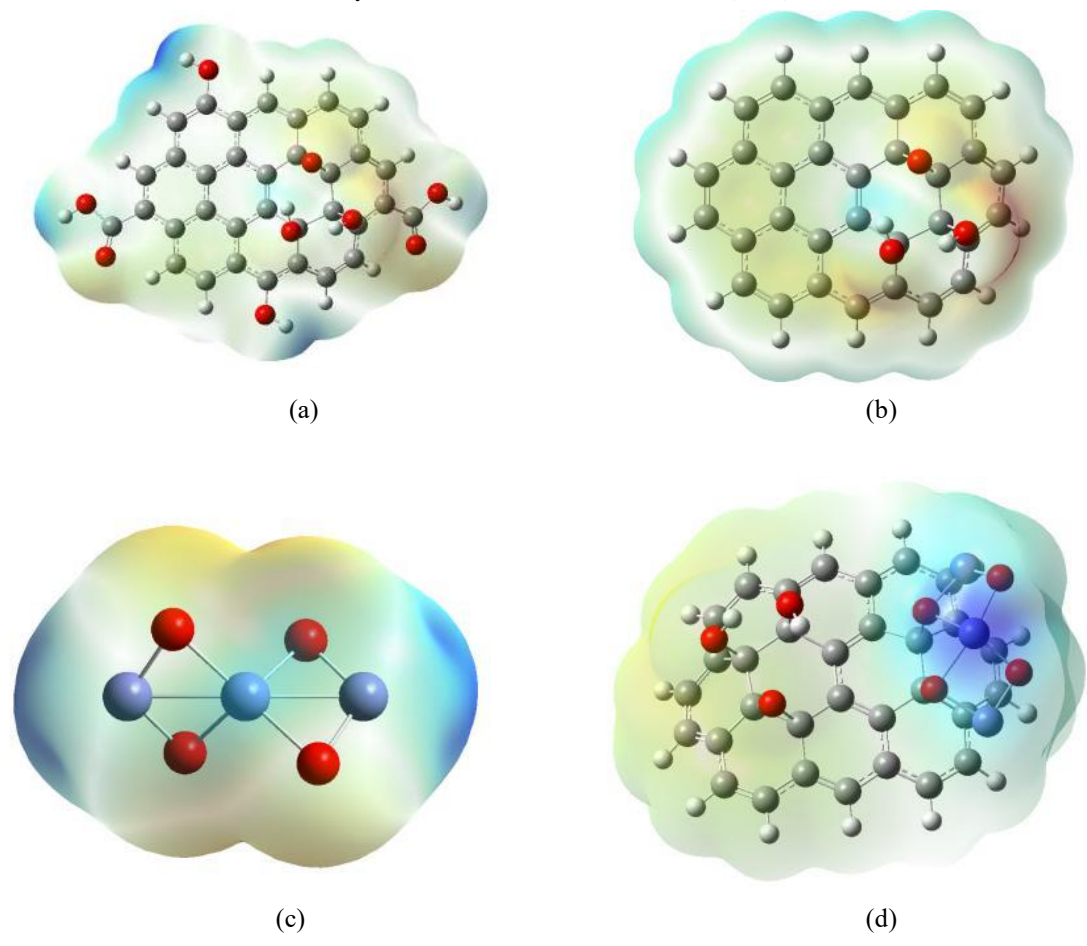


**Figure 4.** DFT calculated molecular electrostatic potential (MEP) maps of (a) GO, (b) rGO, (c) MNP and (d) rGO-MNP using B3LYP/6-31G(d,p) and GEN (LANL2DZ) for metal atom

crucial for catalytic activity because it facilitates the adsorption and activation of oxygen molecules.

Figure 4(d) shows why the DFT-calculated MEP map of the rGO-MNP composite exhibits superior catalytic properties for the ORR than its components, rGO and MNP. The MEP map of rGO-MNP shows a highly polarized surface with distinct electron-rich (negative potential) and electron-deficient (positive potential) sites, marked by red and blue regions, respectively. The negative potential regions are associated with oxygen-containing functional groups and reduced graphene oxide surface, providing electron-rich sites for oxygen molecule adsorption. The positive potential regions are primarily associated with the Fe atoms in the magnetite nanoparticles, indicating electron-deficient sites. The composite exhibits a synergistic effect, combining the properties of rGO and MNP and enhancing electrostatic potential distribution. The presence of MNPs introduces additional positive potential regions, crucial for attracting and activating oxygen molecules, while rGO contributes electron-rich sites that facilitate the reduction process. Intermediate regions (yellow and green) represent areas of balanced electron density, essential for stabilizing reaction intermediates during ORR, providing a supportive environment for sequential reaction steps such as O<sub>2</sub> adsorption, O-O bond cleavage, and formation of water or hydroxide ions.

Combining rGO and MNP results in more effective active sites for oxygen molecule adsorption and subsequent reduction steps, which enhances the overall catalytic efficiency. The presence of magnetite nanoparticles improves charge transfer capabilities, facilitating electron transfer to adsorbed oxygen molecules and promoting the reduction process. Additionally, the structural integration of rGO and MNP provides mechanical stability and prevents nanoparticle aggregation, ensuring a more uniform distribution of active sites and consistent catalytic performance. The effectiveness of the rGO-MNP composite in ORR is evident as the electron-rich sites facilitate the initial adsorption of oxygen molecules, and the electron-deficient sites help weaken the O-O

bond, facilitating its cleavage into atomic oxygen or other intermediates. The presence of rGO and MNP ensures efficient electron transfer throughout the composite, reducing adsorbed oxygen intermediates to final products, such as water or hydroxide ions. The rGO-MNP composite exhibits a highly polarized surface with a mix of electron-rich and electron-deficient sites, enhanced charge transfer capabilities, and improved stability, making it a superior catalyst for the oxygen reduction reaction compared to rGO and MNP alone.

In summary, the color-coded MEP maps visually represent the electrostatic potential distribution across the molecular surface. The blue, red, yellow, and green regions in rGO-MNP and other structures indicate areas of varying electron density, which play a crucial role in determining their catalytic properties and interactions with reactants during the ORR.

#### Conclusion

In this study, we explored the electronic and structural properties of rGO-MNP and their potential as catalysts for the ORR using DFT. Geometry optimization revealed significant structural stability and minimal deformation upon adsorption of reactants, indicating a stable hybrid structure conducive for catalytic applications. The substantial binding energies indicated strong adsorption of reactants, essential for efficient catalysis, while favourable interaction energies highlighted the synergistic effect of the composite structure, enhancing the electronic properties of the rGO-MNP. Dipole moment analysis indicated significant charge separation within the composite, facilitating electron transfer during ORR. Frontier Molecular Orbitals (HOMO and LUMO) analysis revealed a suitable energy gap for electron transfer processes and efficient charge transfer pathways, essential for catalytic activity. MEP maps indicated regions of high electron density likely to be active sites for ORR. Collectively, these findings demonstrate that rGO-MNP holds significant promise as an efficient catalyst for ORR, with strong capabilities, favourable adsorption interaction energies, appropriate dipole moments, advantageous electronic properties. Future work could involve experimental validation of these theoretical predictions and exploring the scalability of rGO-MNP synthesis for practical applications in energy conversion and storage devices. This comprehensive DFT study provides valuable insights into the catalytic potential of rGO-MNP and lays a solid foundation for further exploration and development of advanced nanomaterials for energy-related applications.

### Acknowledgements

The authors express their gratitude to the Ministry of Higher Education (MOHE) for providing financing under the Fundamental Research Grant Scheme FRGS/1/2021/STG04/UMT/02/1. We are also grateful for the research facilities provided by the Universiti Malaysia Terengganu's Central Lab and by Universiti Teknologi Malaysia.

#### References

- Vinogradov, K. Y., Bulanova, A. V., Shafigulin, R. V., Tokranova, E. O., Mebel, A. M., and Zhu, H. (2022). Density functional theory study of the oxygen reduction reaction mechanism on graphene doped with nitrogen and a transition metal. ACS Omega, 7(8): 7066-7073.
- 2. Yusoff, F., Suresh, K., and Khairul, W. M. (2022). Synthesis and characterization of reduced graphene oxide/iron oxide/silicon dioxide (rGO/Fe<sub>3</sub>O<sub>4</sub>/SiO<sub>2</sub>) nanocomposite as a potential cathode catalyst. *Journal of Physics and Chemistry of Solids*, 163, 110551.
- 3. Tyagi, A., et al. (2021). ORR performance evaluation of Al-substituted MnFe<sub>2</sub>O<sub>4</sub>/reduced graphene oxide nanocomposite. International *Journal of Hydrogen Energy*, 46(43): 22434-22445.
- 4. Kattel, S., Atanassov, P., and Kiefer, B. (2014). A density functional theory study of oxygen reduction reaction on non-PGM Fe-Nx-C electrocatalysts. *Physical Chemistry Chemical Physics*, 16(27): 13800-13806.
- 5. Kreps, B. H. (2020). The rising costs of fossil-fuel extraction: An energy crisis that will not go away. *American Journal of Economics and Sociology*, 79(3): 695-717.
- Jin, N., Han, J., Wang, H., Zhu, X., and Ge, Q. (2015). A DFT study of oxygen reduction reaction mechanism over O-doped graphene-supported Pt4, Pt3Fe and Pt3V alloy catalysts. *International Journal of Hydrogen Energy*, 40(15): 5126-5134.
- Muhamad, N. B., and Yusoff, F. (2018). The physical and electrochemical characteristic of gold nanoparticles supported PEDOT/graphene composite as potential cathode material in fuel cells. *Malaysian Journal of Analytical Sciences*, 22(6): 921-930.
- Jagdale, P. B., Manippady, S. R., Anand, R., Lee, G., Samal, A. K., Khan, Z., and Saxena, M. (2024). Agri-waste derived electroactive carbon-iron oxide nanocomposite for oxygen reduction reaction: An experimental and theoretical study. RSC Advances, 14(17): 12171-12178.
- 9. Nørskov, J. K., Rossmeisl, J., Logadottir, A., Lindqvist, L. R. K. J., Kitchin, J. R., Bligaard, T., and Jonsson, H. (2004). Origin of the overpotential for oxygen reduction at a fuel-cell cathode. *Journal of Physical Chemistry B*, 108(46): 17886-17892.

- Bhatt, M. D., Lee, G., and Lee, J. S. (2017). Density functional theory (DFT) calculations for oxygen reduction reaction mechanisms on metal-, nitrogen-co-doped graphene (M-N2-G (M = Ti, Cu, Mo, Nb and Ru)) electrocatalysts. *Electrochimica Acta*, 228: 619-627.
- 11. Al-Bagawi, A. H., Bayoumy, A. M., and Ibrahim, M. A. (2020). Molecular modeling analyses for graphene functionalized with Fe3O4 and NiO. *Heliyon*, 6(7), e04456.
- 12. Zhuo, H. Y., Zhang, X., Liang, J. X., Yu, Q., Xiao, H., and Li, J. (2020). Theoretical understandings of graphene-based metal single-atom catalysts: Stability and catalytic performance. *Chemical Reviews*.
- 13. Yusoff, F., Rosli, A. R., and Ghadimi, H. (2021). Synthesis and characterisation of gold nanoparticles/poly3,4-ethylene-dioxythiophene/reduced-graphene oxide for electrochemical detection of dopamine. *Journal of the Electrochemical Society*, 168(2): 026509.
- Ding, R., Zhang, J., Qi, J., Li, Z., Wang, C., and Chen, M. (2018). N-doped dual carbon-confined 3D architecture rGO/Fe<sub>3</sub>O<sub>4</sub>/AC nanocomposite for high-performance lithium-ion batteries. ACS Applied Materials & Interfaces, 10(16): 13470-13478.
- Haris, N. S. H., Mansor, N., Mohd Yusof, M. S., Sumby, C. J., and Abdul Kadir, M. (2021). Investigating the potential of flexible and preorganized tetraamide ligands to encapsulate anions in one-dimensional coordination polymers: Synthesis, spectroscopic studies and crystal structures. Crystals (Basel), 11(1): 1-14.
- Sheikhi, M., Balali, E., and Lari, H. (2016). Theoretical investigations on molecular structure, NBO, HOMO-LUMO and MEP analysis of two crystal structures of N-(2benzoyl-phenyl) oxalyl: A DFT study. *Journal* of Physical and Theoretical Chemistry, 13: 155-171.
- Jiang, B., Li, L., Zhang, Q., Ma, J., Zhang, H., Yu, K., and Tang, D. (2021). Iron–oxygen covalency in perovskites to dominate syngas yield in chemical looping partial oxidation. *Journal of Materials Chemistry A*, 9(22), 13008– 13018.
- Catlow, C. R. A., Guo, Z. X., Miskufova, M., Shevlin, S. A., Smith, A. G. H., Sokol, A. A., ... and Woodley, S. M. (2010). Advances in computational studies of energy materials. *Philosophical Transactions of the Royal Society* A: Mathematical, Physical and Engineering Sciences, 368(1923): 3495-3511.

- 19. Karimi-Maleh, H., Shafieizadeh, M., Taher, M. A., Opoku, F., Kiarii, E. M., Govender, P. P., ... and Orooji, Y. (2020). The role of magnetite/graphene oxide nano-composite as a high-efficiency adsorbent for removal of phenazopyridine residues from water samples: An experimental/theoretical investigation. *Journal of Molecular Liquids*, 298: 112040.
- Singh, S. K., Takeyasu, K., and Nakamura, J. (2019). Active sites and mechanism of oxygen reduction reaction electrocatalysis on nitrogendoped carbon materials. *Advanced Materials*, 31(27): 1804297.
- 21. Kabir, S., Artyushkova, K., Serov, A., Kiefer, B., and Atanassov, P. (2016). Binding energy shifts for nitrogen-containing graphene-based electrocatalysts: Experiments and DFT calculations. *Surface and Interface Analysis*, 48(5): 293-300.
- 22. Galano, A., and Alvarez-Idaboy, J. R. (2006). A new approach to counterpoise correction to BSSE. *Journal of Computational Chemistry*, 27(11): 1203-1210.
- 23. Ketmen, S., Zeybekler, S. E., Gelen, S. S., and Odaci, D. (2022). Graphene oxide-magnetic nanoparticles loaded polystyrene-polydopamine electrospun nanofibers based nanocomposites for immunosensing application of C-reactive protein. *Biosensors (Basel)*, 12(12): 1175.
- 24. Covarrubias-García, I., Quijano, G., Aizpuru, A., Sánchez-García, J. L., Rodríguez-López, J. L., and Arriaga, S. (2020). Reduced graphene oxide decorated with magnetite nanoparticles enhances biomethane enrichment. *Journal of Hazardous Materials*, 397: 122760.
- 25. Lellala, K. (2021). Microwave-assisted facile hydrothermal synthesis of Fe<sub>3</sub>O<sub>4</sub>-GO nanocomposites for the efficient bifunctional electrocatalytic activity of OER/ORR. *Energy & Fuels*, 35(9): 8263-8274.
- Shpilman, J. S., Friedman, A., Zion, N., Levy, N., Major, D. T., and Elbaz, L. (2019). Combined experimental and theoretical study of cobalt corroles as catalysts for oxygen reduction reaction. *Journal of Physical Chemistry C*, 123(50): 30129-30136.
- 27. Islam, M. A., Hossain, M. S., Hasnat, S., Shuvo, M. H., Akter, S., Maria, M. A., ... and Hoque, M. N. (2024). In-silico study unveils potential phytocompounds in Andrographis paniculata against E6 protein of the high-risk HPV-16 subtype for cervical cancer therapy. *Scientific Reports*, 14(1): 65112.